Recent Development of Road Condition Estimation Techniques for Electric Vehicle and their Experimental Evaluation using the Test EV "UOT March I and II"

Kimihisa Furukawa
Department of Electrical Engineering
The University of Tokyo
Ce-503, 4-6-1 Komaba, Meguro, Tokyo
153-8505 Japan
Tel: +81-3-5452-6289, Fax: +81-3-5452-6288
E-mail: furukawa@horilab.iis.u-tokyo.ac.jp

Yoichi Hori
Institute of Industrial Science
The University of Tokyo
Ce-501, 4-6-1 Komaba, Meguro, Tokyo
153-8505 Japan
Tel: +81-3-5452-6287, Fax: +81-3-5452-6288
E-mail: hori@iis.u-tokyo.ac.jp, y.hori@ieee.org

***Abstract*— In this paper, the latest developed results are described about road surface condition estimation for Electric Vehicles (EVs). The road surface condition, represented by "frictional coefficient vs. slip ratio" characteristics, is the most important information for advanced vehicle control, like active safety system. In Hori laboratory, various road surface condition estimation techniques have been proposed using driving-force observer. This observer is based on one of the excellent features of EVs, i.e., motor torque can be known easily and precisely from motor current. First, the principle of the driving-force observer is explained. Next, the road surface condition estimation techniques, μ gradient, $\mu_{\rm peak}$ and $\lambda_{\rm opt}$ estimation techniques are introduced. At last, applications of these estimation techniques are shown and confirmed using experimental EVs "UOT March I and II".**

I. Introduction

In these days, Electric Vehicles (EVs) attract attention as one of environment-friendly technologies. However, researches on motion control for EVs are not so well developed, although it can utilize the most remarkable merit of electric motor [1][2][3][4].

We have pointed out the following three advantages of EVs:

1) *Motor torque can be known easily and precisely from motor current.*
2) *Motor torque generation is very quick and accurate.*
3) *Motor can be installed in each wheel.*

In Hori laboratory, many researches to use these merits of EVs are done and verified by the experimental EVs "UOT (University of Tokyo) March I and II". UOT March II can be used for two-dimensional motion control experiment. An in-wheel motor is installed in each wheel, and the torque of each wheel can be controlled with full independence [2][3][5].

In this paper, road surface condition estimation techniques are introduced using the advantage of 1) [6]. The road surface condition estimation is an important technique for active safety systems. In past researches, it is well known that driving-force between tire and road has significant information. For Internal Combustion Vehicles (ICVs), direct estimation is impossible using driving-force information because observation of generated engine torque is difficult. On the contrary, in the case of EVs, the estimation using driving-force observer is possible because it is easy to monitor generated motor torque.

Next, the road surface condition estimation techniques and their experimental results with "UOT March I" are shown. Section II describes frictional characteristics between tire and road. In section III, the driving-force observer, which is utilizing the advantage of EVs, is introduced. In section IV, two kinds of road surface condition estimation techniques are introduced. First, μ gradient estimation technique (IV-A) is explained as the most basic estimation algorithm using only μ and λ information. Second, $\mu_{\rm peak}$ and $\lambda_{\rm opt}$ estimation techniques (IV-B) based on characteristics of μ-λ curve are introduced. In section V, applications of the road surface condition estimation techniques are shown.

(a) External appearance of "UOT March II"

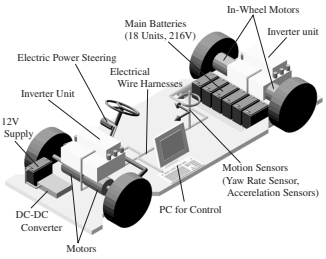

(b) Configuration of "UOT March II"

Fig. 1. Our handmade Experimental EV "UOT March II"

II. Frictional characteristics between tire and road

In this section, frictional characteristics are shown between tire and road surface which are the fundamental concept of the road surface condition estimation [7][8].

Driving-force is generated by velocity difference between vehicle and wheel, i.e., the slip velocity. Vehicle behavior is decided by driving-force F_d shown in Fig. 2(a). As shown in (1) driving-force is given by using frictional coefficient μ and normal force N.

$$F_d = \mu(\lambda)N \tag{1}$$

Frictional coefficient μ is the function of slip ratio λ shown in Fig. 2(b), and this curve is called μ-λ curve. Slip ratio is given by using chassis velocity V and wheel velocity V_w as (2).

$$\lambda = \frac{V_w - V}{\max(V, V_w)} \tag{2}$$

The performance of driving-force is affected by the relationship between μ and λ, which has non-linear characteristics with peak value $\mu_{\rm peak}$ (hereinafter referred to as peak frictional coefficient). The slip ratio $\lambda_{\rm opt}$ (hereinafter referred to as

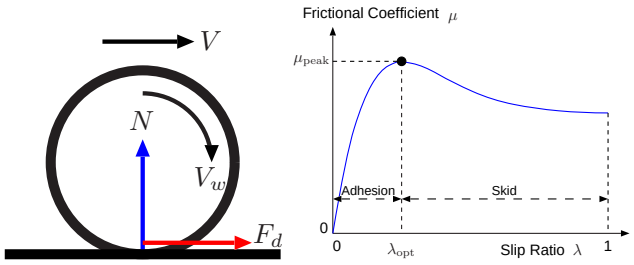

(a) Driving force between tire and road in one wheel model

(b) Characteristics of μ-λ curve

Fig. 2. The schematic of one wheel model and the characteristic illustration of μ-λ curve

optimal slip ratio) where frictional coefficient has μ_{peak}, is usually from 0.05 to 0.2.

In adhesion state: $\lambda \leq \lambda_{\text{opt}}$, vehicle is in stable because the condition between tire and road is in adhesive. In skid state: $\lambda > \lambda_{\text{opt}}$, the wheel is accelerated and big spin occurs.

The road surface condition estimation is used for the purpose of holding vehicle motion stability le. In other words, it estimates the stability limit between adhesion and skid states when the vehicle is in adhesion.

III. Driving-Force Observer

The information of frictional coefficient μ is indispensable for road surface condition estimation. As it was shown in (1), frictional coefficient is obtained by driving-force F_d and normal force N. However it is impossible to observe directly driving-force generated between tire and road, therefore observer is needed to estimate driving-force. In this section, the principle of driving-force observer is briefly explained [9].

In electric motor, generated torque can be monitored precisely and easily, therefore it is possible for EVs to estimate driving-force with high precision. In the case of EVs, motor current and wheel velocity, which are needed to calculate generated torque, can be measured. Actually, armature current in a DC motor or torque current in an AC motor is used. The dynamic equations about a driving wheel (3) and a chassis (4) are derived from one wheel vehicle model shown in Fig. 3,

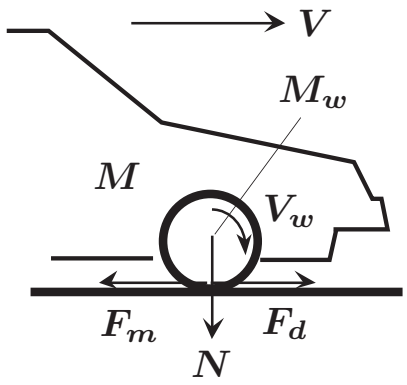

Fig. 3. The schematic of one wheel vehicle model

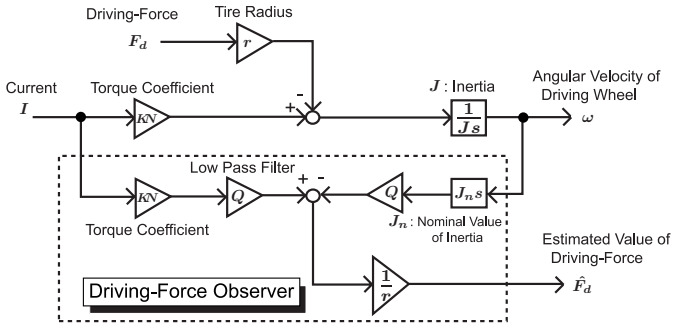

Fig. 4. Block diagram of the driving-force observer

$$M_w \frac{dV_w}{dt} = F_m - F_d \tag{3}$$

$$M \frac{dV}{dt} = F_d \tag{4}$$

where, M_w is wheel inertia converted to mass, F_m is motor torque converted to force, F_d is driving-force and M is vehicle body mass.

The dynamic equation of driving wheel shown in (3) is used to derive driving-force as (5),

$$F_d = \frac{1}{r}(T - J\frac{d\omega}{dt}) \tag{5}$$

where, r is radius of wheel, T is motor torque, J is wheel inertia and ω is angular velocity of driving wheel. These values are related with F_m, M_w, and V_w respectively as follows.

$$F_m = T/r, \quad M_w = J/r^2 \text{ and } V_w = r\omega \tag{6}$$

Based on (5), the block diagram of the driving-force observer is shown in Fig. 4. The figure is for a shunt DC motor case, $\hat{F}_d$, K, N, and J_n are the estimated driving-force, the torque coefficient, the gear ratio of transmission, and the nominal value of wheel inertia respectively. This is called driving-force observer, though this structure is the same as disturbance observer often used in mechatronics.

The observer uses first order derivative of ω, which induces higher frequency noise from differential operation. Therefore, low pass filters "Q" are needed.

IV. Road Surface Condition Estimation Using Driving-Force Observer

The road surface condition estimation based on the driving-force observer is one of the merits of EVs. In this section the road surface condition estimation techniques for EVs proposed in Hori Laboratory are introduced.

A. Basic estimation techniques based only on μ and λ (i.e., μ gradient ($d\mu/d\lambda$) estimation)

By using μ gradient, the frictional characteristics between tire and road can be known. For example, feedback control to maintain μ gradient to be 0 is effective to increase adhesion. In this term, results of identification by fixed trace method (FT) are shown, and they are evaluated which approach is more useful [9].

μ gradient ($= d\mu/d\lambda$) can be estimated with frictional coefficient μ and slip ratio λ. They can be detected by the driving-force observer and wheel velocity respectively. The chassis velocity required for slip ratio calculation is obtained

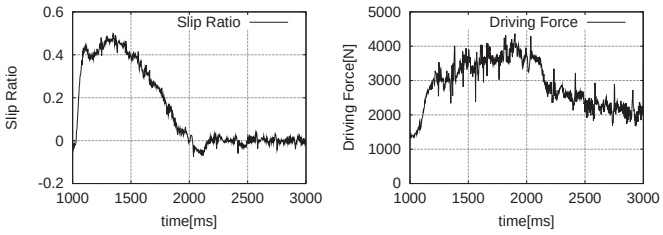

(a) Slip ratio (b) Estimated driving-force

Fig. 5. Experimental data on asphalt road

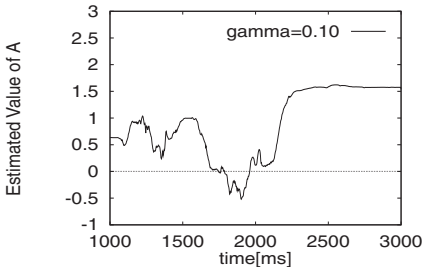

Fig. 6. Result of μ gradient estimation (asphalt, $\gamma = 0.10$)

by non-motored wheel velocity. Estimated μ gradient is used as follows. A wheel spin can be detected by μ gradient characteristics because μ gradient is positive in adhesion state, and negative in skid state. Adhesion control becomes possible using feedback control to regulate μ gradient to be zero.

μ gradient is obtained by (7). To apply adaptive identification (e.g., Fixed Trace (FT) method) for μ gradient estimation, (7) is transformed as (8).

$$A = \frac{d\mu}{d\lambda} = \frac{d\mu/dt}{d\lambda/dt} \tag{7}$$

$$\frac{d\mu}{dt} = A\frac{d\lambda}{dt} \tag{8}$$

To identify linear characteristics represented by (9), algorithm of adaptive identification (recursive least-squares (RLS) method) is applied as (10)-(11), which are recursive equation with forgetting factor κ.

$$y[k] = \hat{\theta}^T[k]\phi[k] \tag{9}$$

$$\hat{\theta}[k] = \hat{\theta}[k-1] - \frac{P[k-1]\phi[k]}{1+\phi^T[k]P[k-1]\phi[k]} *(\hat{\theta}[k-1]\phi[k] - y[k]) \tag{10}$$

$$P[k] = \frac{1}{\kappa}\left[P[k-1] - \frac{P[k-1]\phi[k]\phi^T[k]P[k-1]}{1+\phi^T[k]P[k-1]\phi[k]}\right] \tag{11}$$

In the case of Fixed Trace (FT) method, trace gain $\gamma = \mathrm{tr}P[k]$ is fixed. Especially, in the 1st dimension FT method, forgetting factor κ is given by (12),

$$\kappa = \frac{1}{1+\gamma\|\phi[k]\|^2} \tag{12}$$

where, each variable of (9) is set as (13) based on (8).

$$\phi[k] = \frac{d\lambda}{dt}, \quad y[k] = \frac{d\mu}{dt}, \quad \hat{\theta}[k] = \hat{A} \tag{13}$$

In comparison with RLS, FT method uses variable forgetting factor κ because trace gain $\gamma = \mathrm{const.}$ as (12). In other words, when $\phi[k]$ is big and $\hat{\theta}$ can be identified with good precision, $\hat{\theta}$ is updated in a short time. Whereas, when $\phi[k]$ is small and not of "rich" information, $\hat{\theta}$ is seldom updated.

μ gradient is estimated using experimental data of "UOT March I" to confirm the performance of FT method explained as above.

First, an estimation result is shown Fig. 6 based on an asphalt data (Fig. 5). In Fig. 6, trace gain is $\gamma = 0.10$. In principle, μ gradient estimation around $d\lambda/dt \simeq 0$ is physically impossible. By utilizing FT method, a stable estimation is realized in $d\lambda/dt \simeq 0$, because the forgetting factor is almost 1 and past estimated value can be kept.

Precision, stability and delay of estimation depend on the values of κ and γ. These parameters must be adjusted corresponding to road surface condition.

B. Advanced estimation techniques using μ-λ relation

1) μ_{peak} estimation based on tire model: The tire model proposed by Dr. Yamazaki says that the value of μ gradient near $\lambda = 0$ includes the information of peak frictional coefficient μ_{peak} [10]. Therefore, the value of μ_{peak} can be estimated by the data of driving-force, wheel velocity around $\lambda = 0$ and typical characteristics of μ-λ curve. This technique is very useful to prevent big skidding [6].

First, a physical analysis about the frictional characteristics between tire and road is given. On tire tread, adhesive and sliding area are mixed. The proportion of two areas changes depending on the slip ratio as shown in Fig. 7. This phenomenon is analyzed based on the brush model (see Fig. 8(a)). The distribution of ground contact pressure in tire tread is assumed as parabolic shape shown in Fig. 8(b). Ground contact pressure p is given as (14) using maximum ground contact pressure p_m, and ground contact length, l.

$$p = 4p_m\frac{\xi}{l}(1-\frac{\xi}{l}) \tag{14}$$

Normal force of tire tread, N, is given by (15) using ground contact width.

$$N = \frac{2}{3}p_m w l \tag{15}$$

In adhesive area, friction stress $\sigma_\xi^{(a)}$, which is decided by shearing stress, is given by (16) using longitudinal spring constant of tread rubber for each unit area. In sliding area, friction stress $\sigma_\xi^{(s)}$, which is decided by peak frictional coefficient

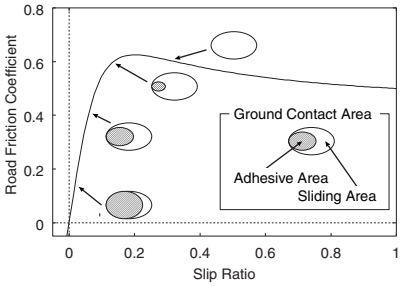

Fig. 7. Variation of adhesive and sliding areas

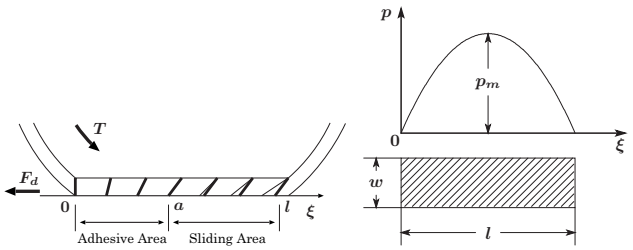

(a) Tire brush model (b) Distribution of ground pressure

Fig. 8. Physical configuration of tire tread

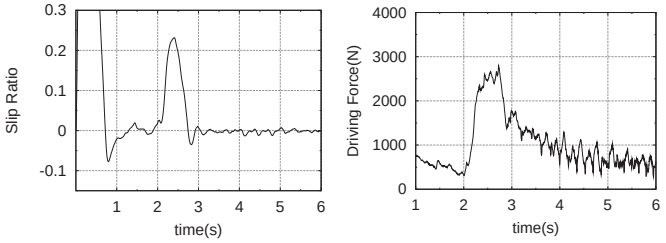

(a) Slip ratio (b) Estimated driving-force

Fig. 9. Experimental data on asphalt road

$\mu_{\rm peak}$, is given by (17).

$$\sigma_\xi^{(a)} = k_x \lambda \xi \tag{16}$$

$$\sigma_\xi^{(s)} = \mu_{\rm peak} p \tag{17}$$

The friction stresses take the same value at the boundary between adhesive and sliding area represented by $\xi = a$,

$$\sigma_a^{(a)} = \sigma_a^{(s)}. \tag{18}$$

Driving-force F_d is given by (19),

$$\begin{aligned} F_d &= \int_0^l \sigma_\xi w d\xi \\ &= \int_0^a \sigma_\xi^{(a)} w d\xi + \int_a^l \sigma_\xi^{(s)} w d\xi \\ &= C_s \lambda - \frac{(C_s\lambda)^2}{3\mu_{\rm peak} N} + \frac{(C_s\lambda)^3}{27(\mu_{\rm peak} N)^2} \end{aligned} \tag{19}$$

where, driving stiffness C_s, which is the driving-force for unit slip ratio at $\lambda = 0$, is given by (20).

$$C_s = \frac{1}{2} w k_x l^2 \tag{20}$$

The solution of the maximum driving-force, $\mu_{\rm peak} N$, from (19) is obtained as (21).

$$\mu_{\rm peak} N = \frac{3(C_s\lambda)^2 + \sqrt{3(C_s\lambda)^3(4F_d - C_s\lambda)}}{18(C_s\lambda - F_d)} \tag{21}$$

As measured signals contain much noise, $\mu_{\rm peak}$ estimation is difficult if (21) is directly applied. Therefore, estimation algorithms same as (9)-(11) used in IV-A is applied. $y[k]$, $\phi[k]$ and $\theta[k]$ take the forms of (22)-(24).

$$y[k] = 3(C_s\lambda)^2 + \sqrt{3(C_s\lambda)^3(4F_d - C_s\lambda)} \tag{22}$$

$$\hat{\theta}[k] = \mu_{\rm peak} N \tag{23}$$

$$\phi[k] = 18(C_s\lambda - F_d) \tag{24}$$

To confirm the validity of the introduced technique, road surface condition is estimated in off-line calculation using the data measured by the experimental EV "UOT March I".

The experimental data in dry asphalt road are shown in Fig. 9. In this experiment, the vehicle is accelerated at 2 sec. Hence, slip ratio grows bigger immediately by urgent acceleration. The estimation result of maximum driving-force is shown in Fig. 10.

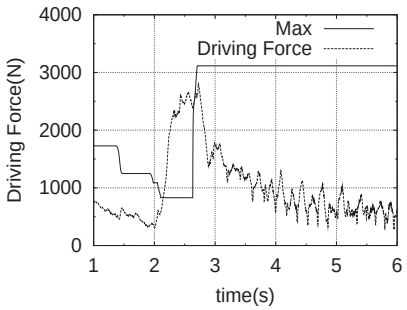

Fig. 10. Result of the $\mu_{\rm peak}$ estimation

2) $\lambda_{\rm opt}$ estimation based on geometric similarity of μ-λ curve: To estimate optimal slip ratio, λ_{opt}, we use the information of μ, λ and μ gradient. However, this information contains much noise and error, too, stable estimation is difficult in search algorithm such as gradient method.

In this section, as a robust optimal slip ratio estimation Fuzzy inference is introduced [8].

One of the characteristics of the μ-λ curve, optimal slip ratio $\lambda_{\rm opt}$ has strong relation with μ gradient (see Fig. 11, A_1 and A_2 represent μ gradient). This geometrical characteristics can be applied to $\lambda_{\rm opt}$ estimation.

This characteristic is proved in μ-λ curves which have same $\mu_{\rm peak}$. We do not need so accurate $\mu_{\rm peak}$ value. Then, we need similarity information of $\mu_{\rm peak}$ with four kinds of standard road surface conditions, ASPHALT, GRAVEL, SNOW and ICE, which are displayed in Fig. 12.

Using μ and λ values, degrees of similarity to the standard road surface conditions are obtained numerically by Fuzzy

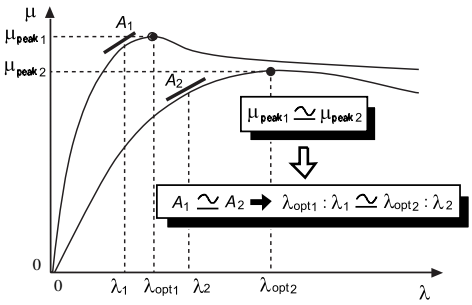

Fig. 11. Geometrical characteristics of μ-λ curves

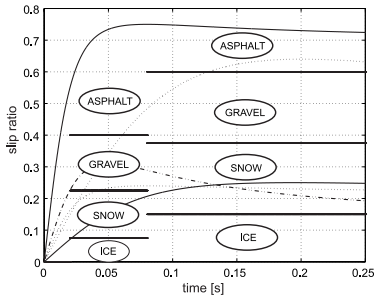

Fig. 12. The schematic about the classification of road surface conditions

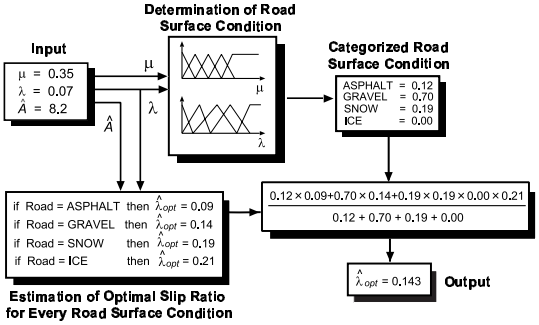

Fig. 13. Block diagram of optimal slip ratio estimator

inference.

In optimal slip ratio estimation, we need two kinds of algorithms. 1st algorithm is to obtain road surface condition similarities with four kinds of standard road surface conditions, described as above. 2nd algorithm is $\lambda_{\rm opt}$ estimation to the standard road surface conditions with Fuzzy inference. This estimation uses estimated μ gradient, $\hat{A}$, and λ based on geometrical characteristics.

The block diagram of optimal slip ratio estimator is shown in Fig. 13. Using information from these algorithms, $\lambda_{\rm opt}$ is obtained by (25). Estimated optimal slip ratios to each standard road, $\hat{\lambda}_{opt_A}$, $\hat{\lambda}_{opt_G}$, $\hat{\lambda}_{opt_S}$, and $\hat{\lambda}_{opt_I}$ are weighted by K_A, K_G, K_S, and K_I respectively, which are road surface condition similarities with standard road surface conditions.

$$\hat{\lambda}_{opt} = \frac{K_A\hat{\lambda}_{opt_A}+K_G\hat{\lambda}_{opt_G}+K_S\hat{\lambda}_{opt_S}+K_I\hat{\lambda}_{opt_I}}{K_A+K_G+K_S+K_I} \tag{25}$$

The estimated result by this technique will be shown in V-B.

V. Application of the Road Surface Condition Estimation

A. Indication of adhesion rate to driver

If the car tells the driver "Our car has entered snowy road", it must be a great help for vehicle safety. The $\mu_{\rm peak}$ estimation technique realizes this function [6].

The technique for $\mu_{\rm peak}$ estimation before entering skid state was proposed in IV-B.1. The ratio of present driving-force to estimated maximum driving-force can be used as the information of adhesion state between tire and road. The adhesion rate r is defined as (26).

$$r = \frac{\hat{F}_d}{\mu_{\rm peak}N} \tag{26}$$

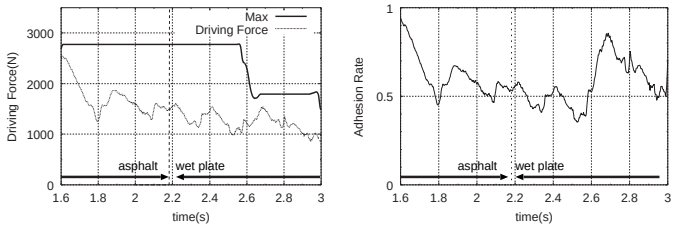

(a) Estimated maximum driving-force

(b) Indicated adhesion rate

Fig. 14. Estimation result of driving-force and adhesion rate when road surface condition changes suddenly

In (26), $\hat{F}_d$ and $\mu_{\rm peak}N$ are obtained by the driving-force observer and peak frictional coefficient estimator respectively.

Adhesion state between tire and road can be quantitatively presented to driver by showing r . In the case that r is low, the state of tire is kept in adhesive if wheel is accelerated further more. Meanwhile, in the case that r approaches 1, the possibility of skidding is high even if wheel is accelerated a little.

Driving-force and adhesion rate when vehicle runs from dry asphalt road to wet iron plate suddenly is shown in Fig. 14. On dry asphalt road, r is about 0.5 and the vehicle is in safe state. While, on wet iron plate, r is rapidly up to about 0.8 shown in Fig. 14. It is possible to inform quantitatively how easy to skid caused by sudden change in road surface condition even if the driving-force is kept almost constant as shown in Fig. 14(a)

B. Optimal slip ratio control

Slip ratio can be maintained to commanded value by strong feedback control. As driving-force is affected by highly non-linear frictional characteristics between tire and road, real-time generation of optimal slip ratio is necessary while vehicle is moving (see IV-B.2).

The technique of optimal slip ratio control, which makes λ follow up $\lambda_{\rm opt}$ changing in real-time with road surface condition, realizes the maximization of driving-force. To achieve this control, slip ratio control shown in Fig. 15 is applied. $\hat{\lambda}_{\rm opt}$, the estimated $\lambda_{\rm opt}$ using the optimal slip ratio estimator, is set up as the desired value for the slip ratio control. To obtain $\hat{\lambda}_{\rm opt}$, an estimation algorithm based on Fuzzy inference is applied, introduced in IV-B.2. The whole block diagram of the optimal slip ratio control system is shown in Fig. 16 [8].

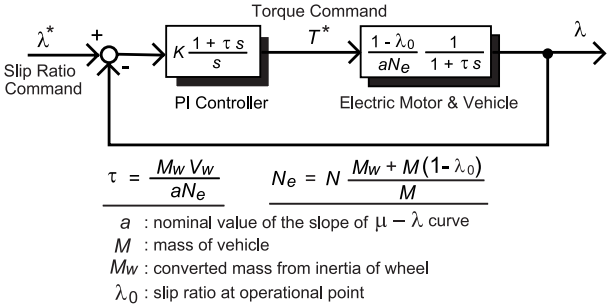

Fig. 15. Block diagram of slip ratio control

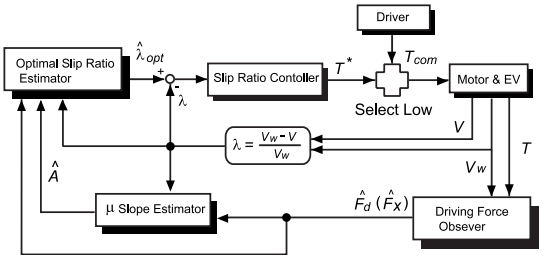

Fig. 16. Whole block diagram of the optimum slip ratio control system

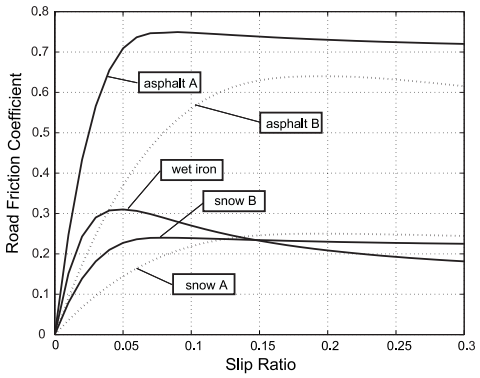

Fig. 17. The schematic of μ-λ curves used in simulation

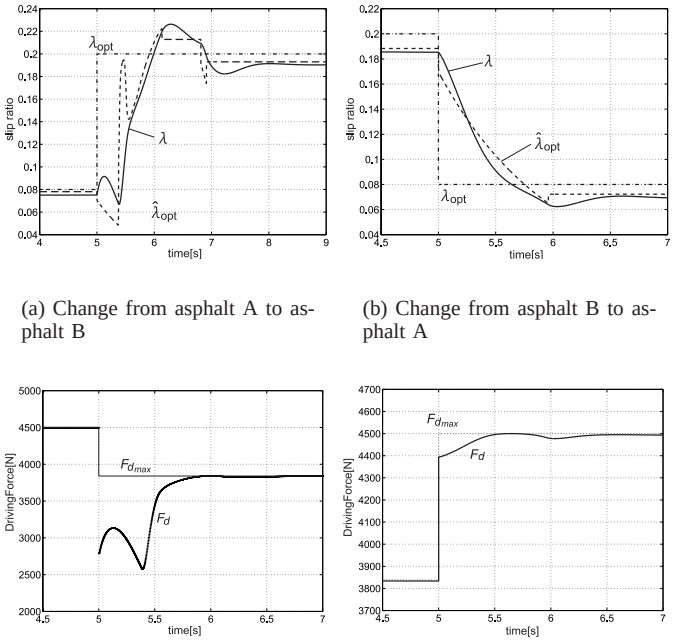

(a) Change from asphalt A to asphalt B

(b) Change from asphalt B to asphalt A

(c) Change of driving-force in case of (a)

(d) Change of driving-force in case of (b)

Fig. 18. Simulation results at the changing road surface condition

Here, cruising simulation is done using the estimation algorithm explained in IV-B.2. The approximated Magic-Formula shown in (27) is applied for μ-λ curve.

$$\mu = C\sin(D\arctan(E\lambda)) \tag{27}$$

Five μ-λ curves which have different $\mu_{\rm opt}$ and $\lambda_{\rm opt}$ are decided by using the experimental data from "UOT March I" for the simulation. These curves are shown in Fig. 17.

Transient response of λ is simulated in the case that vehicle is in full acceleration and the frictional characteristic changed at the moment of 5 sec. Dead-zone is set in $-0.1 < \hat{A} < 0.5$, and Low Pass Filter is inserted into λ and μ to uniform the delay of input signals to each estimator.

Figs. 18(a) and (b) are the estimation results when the road surface condition changes. It takes about 2 sec. to follow up in both case of Figs. 18(a) and (b).

Change in the driving-force of Figs. 18(a) and (b) cases is depicted in Figs. 18(c) and (d). The maximum driving-force is well followed within about 1 sec. This delay is allowable when slippery road, such as snow-covered road, continues for a long time, although it is difficult to estimate a small water pool suddenly appears during cruising even on asphalt road.

VI. Conclusion

In this paper, the road surface condition estimation and its applications have been shown based on the driving force observer. It was realized by using such advantages of electric motor that motor torque can be known easily from motor current. Therefore, these estimations and controls are only realized by EVs. The strong advantages of EVs are in a new field of control and estimation as mentioned in this paper.

References

[1] Y. Hori, "Recent Trends of Electric Vehicle Technology", Japan-China Bilateral Seminar on Transportation Research and Infrastructure Planning in 1998 (JC-TRIP'98), Beijing, 1998.

[2] Y. Hori, "Future Vehicle driven by Electricity and Control - Research on 4 Wheel Motored UOT March II", Proc. of AMC 2002, invited paper, pp.1-14, Maribor, Slovenia, 2002.

[3] S. Sakai, H. Sado and Y. Hori, "Motion Control in an Electric Vehicle with Four Independently Driven In-Wheel Motors", IEEE Trans. on Mechatronics, Vol.4, No.1, pp.9-16, 1999.

[4] H. Shimizu, K. Kawakami, Y. Kakizaki, S. Matsugaura and M. Ohnishi, " "KAZ"The super electric vehicle", Proc. of EVS18, Berlin, 2001.

[5] S. Sakai, T. Okano, C. H. Tai, T. Uchida and Y. Hori, "4 Wheel Motored Vehicle "UOT Electric March II" -Experimental EV for Novel Motion Control Studies-", INTERMAC2001 Joint Technical Conference, Tokyo, 2001.

[6] Y. Hori and K. Furukawa, "Road Surface Condition Estimation and Control utilizing Advantages of Electric Vehicle", 27th Technical Meeting of Control Technology Division, 2nd Symposium of Adaptive and Learning Committee, SICE (Society of Instrumentation and Control Engineers), pp.1-16, 2002, in Japanese.

[7] Y. Hori, Y. Toyoda and Y.Tsuruoka, "Traction Control of Electric Vehicle -Basic Experimental Results using the Test EV UOT Electric March", IEEE Trans. on Industry Applications, Vol.34, No.5, pp.1131-1138, 1998.

[8] H. Kataoka, H. Sado, S. Sakai and Y. Hori, "Optimal Slip Ratio Estimator for Traction Control System of Electric Vehicle based on Fuzzy Inference", The Transactions of The Institute of Electrical Engineers of Japan, Vol.120-D, No.4, pp.581-586, 2000, in Japanese.

[9] H. Sado, S. Sakai and Y. Hori, "Road Condition Estimation for Traction Control in Electric Vehicle", in Proc. of the 1999 IEEE International Symposium on Industrial Electronics, Bled. Slovenia, 99TH8465,Vol.2, pp.973-978, 1999.

[10] S. Yamazaki, "Evaluation of Friction Coefficient between Tire and Road Surface during Running", Journal of Automotive Engineers of Japan, Vol.51, No.11, pp.58-62, 1997, in Japanese.